Dyes and Pigments 175 (2020) 108155

Contents lists available at ScienceDirect

Dyes and Pigments

journal homepage: http://www.elsevier.com/locate/dyepig

Synthetic substituted boronates of dihydroxy-bacteriochlorin absorbing and emitting far-red to near-infrared light as bacteriopheophytin-*a* analogs

Daichi Funakoshi [a], Yosaku Nomura [a], Sunao Shoji [a,b], Hitoshi Tamiaki [a,*]

[a] Graduate School of Life Sciences, Ritsumeikan University, Kusatsu, Shiga, 525-8577, Japan
[b] Division of Applied Chemistry, Faculty of Engineering, Hokkaido University, Sapporo, Hokkaido, 060-8628, Japan

ARTICLE INFO

Keywords:
Chlorophyll-*a*
Fluorescence emission
Qy absorption
Semisynthesis
Substitution effect

ABSTRACT

Several substituted boronates of methyl *cis*-7,8-dihydroxy-pyrobacteriopheophorbide-*a* possessing the same 3-acetyl-13^1-oxo-bacteriochlorin π-conjugated system as bacteriopheophytin-*a* found in type-II reaction centers of anoxygenic photosynthetic bacteria were prepared by chemical modification of chlorophyll-*a*. The semisynthetic bacteriochlorins are less oxidizable to chlorins and more readily available from natural phototrophs than the above natural bacteriochlorin, while the formers show similar optical properties in solution as the latter. All the boronate pigments efficiently absorb near ultraviolet, green, and far-red light and strongly emit light in a far-red to near-infrared region. Their electronic absorption and fluorescence emission data are nearly independent of the alkyl and (hetero)aromatic substituents at the boron atom.

1. Introduction

Anoxygenic photosynthetic bacteria have single charge-separating apparatuses called reaction centers (RCs), which are composed of pigments and peptides. In particular, purple photosynthetic bacteria have pseudo-C_2-symmetric type-II RCs, some of which have been already revealed at an atomic level by crystallographic analyses [1–3]. In the type-II RCs, two bacteriopheophytin(BPhe)-*a* or *b* molecules are found per apparatus, one of which is used as a primary electron acceptor for the photoinduced electron-transfer process. Both BPhe-*a* and *b* pigments possess a bacteriochlorin π-system bearing two single Cβ–Cβ bonds in the opposite pyrrole rings (see Fig. 1, left) [4]. Filamentous anoxygenic phototrophs including green nonsulfur bacteria and Gemmatimonas phototrophs also utilize type-II RCs containing BPhe-*a* [5]. In the RC of the former phototrophs, one extra BPhe-*a* molecule is situated between the primary electron donor (named a special pair) and non-electron-accepting BPhe-*a*.

Naturally occurring bacteriochlorin pigments including BPhes-*a*/*b* are monomeric in conventional organic solvents to give redmost (Qy) absorption bands at around 800 nm in a far-red (FR) to near-infrared (NIR) region. In photosynthetic apparatuses, some of these pigments interact with each other to form dimers and oligomers with bathochromically shifted Qy bands in 800–1100 nm (NIR). Therefore, bacteriochlorins are promising sensitizers for various systems driven by FR-to-NIR light including photodynamic therapy, imaging, and solar cells [6–13]. Natural bacteriochlorins are chemically labile and readily transformed into the corresponding chlorins with a 17,18-dihydroporphyrin π-skeleton to show hypsochromically shifted Qy bands at below 700 nm (a red region). For example, BPhe-*a* is oxidized via the 7,8-didehydrogenation under aerobic conditions and BPhe-*b* is isomerized via hydrogen shift from the C7 to C8^1 position by the action of a weak acid to afford the same 3-acetyl-pheophytin-*a* molecule having a chlorin π-system [14,15]. To enhance the chemical stability of bacteriochlorins, a variety of synthetic analogs have been prepared [16–19]. Thus, Lindsey and his colleagues synthesized nonoxidized and nonisomerized bacteriochlorins based on *gem*-β,β-dimethylpyrrolines [20], and Pandey and his colleagues modified BPhe-*a* to less oxidizable bacteriopurpurinimides [21]. In this context, we previously reported that *cis*-7,8-dihydroxy- [22] and 7,7-dialkyl-8-alkylidne-chlorophyll(Chl)-*a* derivatives [15] were chemically stable and readily available BPhe-*a* and *b* analogs, respectively.

Herein, we report the synthesis of several boronates **1a**–**i** with a less oxidizable bacteriochlorin π-system (Fig. 1, right) by chemically modifying natural Chl-*a*. These synthetic bacteriochlorins exhibit almost the same optical properties in solution, and their electronic absorption and emission data are nearly independent of the substituents (R) on the boron atom. Readily available semisynthetic 3-acetyl-13^1-oxo-bacteriochlorins **1a**–**i** are structurally related to

* Corresponding author.
E-mail address: tamiaki@fc.ritsumei.ac.jp (H. Tamiaki).

https://doi.org/10.1016/j.dyepig.2019.108155
Received 30 September 2019; Received in revised form 17 December 2019; Accepted 18 December 2019
Available online 19 December 2019

natural and fragile BPhe-*a* and, similarly to the latter, intensively absorb and emit light in a FR-to-NIR region. Since a variety of the R groups are easily introduced in the present bacteriochlorins without any alteration of their optical properties, such functionalized boronate pigments are promising for applications including intramolecular electron- and energy-transferring systems from the photoexcited bacteriochlorin moiety to an electron- and energy-donating/accepting moiety in the R group.

2. Results and discussion

2.1. Synthesis of boronates of bacteriochlorin-diol

Naturally occurring Chl-*a* was extracted from cyanobacterial cells and was chemically modified to methyl pyropheophorbide-*a* (**2a**) [step (i) in Scheme 1] [23]. The vinyl group at the 3-position of **2a** was hydrated via a Markovnikov fashion [step (ii)] [23,24], and the resulting 3-(1-hydroxyethyl) group of **2b** was subjected to Ley–Griffith oxidation to give the corresponding 3-acetyl-chlorin, i.e., methyl 7,8-didehydro-pyrobacteriopheophorbide-*a* (**2c**) [step (iii)] [25]. The C7=C8 double bond of **2c** was regioselectively oxidized by osmium tetroxide and the resulting osmate was cleaved by hydrogen sulfide to afford *cis*-7,8-dihydroxy-bacteriochlorin **1j** [step (iv)] [15,26]. In a chlorin π-system, the pyrrole moiety (B-ring) opposite to the reduced pyrrole ring (D-ring) was more reactive than any other adjacent ones (A- and C-rings), so the B-ring was predominantly reacted in the above oxidation. The obtained *cis*-diol **1j** was a 1:1 diastereomeric mixture at the 7,8-positions, namely (7*R*,8*S*)- and (7*S*,8*R*)-stereoisomers. This observation is ascribable to the non-face-selective attack of an OsO_4 species to the C7=C8 moiety far from the chiral (17*S*,18*S*)-positions in a molecule. The stereochemical mixture of **1j** was used for further experiments. It is noted that **1j** is less oxidized to chlorin due to the lack of the 7,8-dihydrogen atoms [22] and also is one of readily accessible bacteriochlorins because the starting material Chl-*a* is easily obtained in large amounts from commercially available spirulina [23].

Next, a dry THF solution of *cis*-diol **1j** was treated with methylboronic acid in the presence of magnesium sulfate as a dehydrating reagent under nitrogen in the dark [step (v) in Scheme 1]. After stirred at room temperature for 1 day, the corresponding methylboronate **1a** was produced, but a part of **1j** yet remained in the reaction mixture. When the reaction mixture was refluxed for 1 day, **1j** was consumed completely, and **1a** was obtained in 80% isolated yield after purification with flash column chromatography (FCC) and recrystallization. Under the same conditions (reflux in THF for 1 day), **1j** partially reacted with dodecylboronic acid to give **1b**, but some **1j** was visible in the reaction mixture. After refluxing at higher temperature in dry toluene for 2 h, **1j** was fully consumed, and **1b** was produced in 90% yield. The difference in the reactivities of methyl- and dodecylboronic acids was most likely due to the greater steric hindrance of the long dodecyl chain than that of the methyl group. In the case of isobutylboronic acid, no esterification occurred upon refluxing in THF for 1 day, and desired **1c** was obtained (81%) after refluxing in toluene for 2 h. The lower reactivity with isobutylboronic acid can be explained by the greater steric bulkiness of the branched primary alkyl group. Isopropylboronic acid could not react with **1j** even after refluxing in toluene for 1 day, which can be ascribed to the presence of the more sterically hindered secondary alkyl group. On the other hand, the reaction of **1j** with cyclopropylboronic acid in toluene afforded desired boronate **1d** in a lower 34% yield after prolonged reflux (1 day). This is ascribable to the less sterically demanding cyclopropyl group which is corresponded to the dehydrogenatively cyclized form of an isopropyl group. Therefore, it can be concluded that the above esterification is largely dependent on the steric factor of the alkyl groups in the boronic acids. The present steric effect is comparable to that for the esterification of a diol with alkyl boronic acids reported previously [27].

Phenylboronic acid readily reacted with **1j** in THF at room temperature to afford phenylboronate **1e** in 77% yield after stirring for 2 days. *p*-Anisylboronic acid was more reactive with **1j** to give **1f** in a higher yield (97%) after stirring at room temperature for a shorter reaction time (1 day). The electron-donating *p*-methoxy group accelerated the esterification. By contrast, the reaction of **1j** with 3,5-bis(trifluoromethyl)phenylboronic acid could not be completed after stirring in THF for 1 day, and harsh reaction conditions (refluxing in toluene for 2 h) were necessary to consume all **1j** and give the corresponding boronate **1g** (78%). The double electron-withdrawing trifluoromethyl groups reduced the esterifying reactivity. Therefore, the acidity of boronic acids affected the above esterification, i.e., the higher acidic boronic acids are, the lower reactive they are with *cis*-diol **1j**. 2,6-Dimethylphenylboronoic acid was so sterically hindered that no esterification with **1j** was observed in THF at room temperature. After refluxing in toluene for 1 day, boronate **1h** was produced (73%). The esterification of **1j** with arylboronic acids was controlled by the steric factor of the aryl group as aforementioned in alkylboronic acids. Additionally, 2-thienylboronic acid reacted with **1j** to give **1i** (51%) after refluxing in toluene for 1 h. Such a heteroaromatic group in the boronic acid was effective for the preparation of boronates of *cis*-diol **1j**. All the synthetic boronates **1a–i** as structural analogs of BPhe-*a* were mixtures of the 7,8-diastereomers as in **1j** (see Fig. 1, right), which were used for the measurements of the following optical properties.

2.2. Electronic absorption properties of boronated bacteriochlorins

Bacteriochlorins have three typical electronic absorption bands, i.e., intense Qy, Qx, and Soret bands, which are situated at 800–700, 600–500, and 400–300 nm, respectively. The Qy and Qx bands are dependent on the transition moments along the molecular y- and x-axes, respectively (see Fig. 2), and the Soret band is composed of By and Bx bands. As shown in Fig. 3, methyl pyrobacteriopheophorbide-*a* (**1k**)

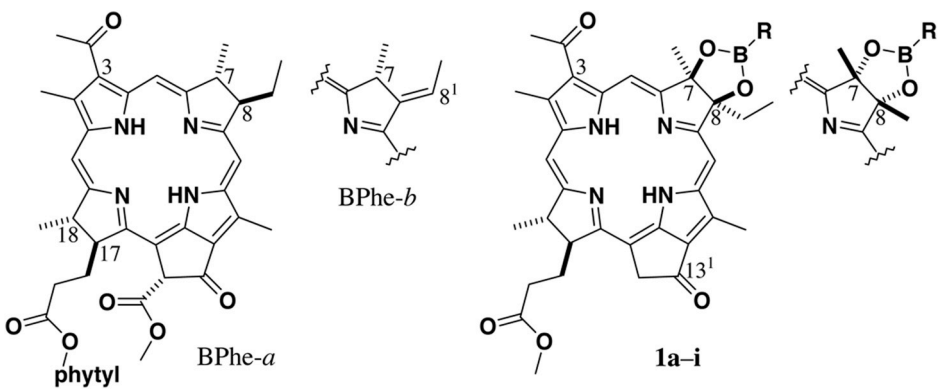

Fig. 1. Molecular structures of naturally occurring bacteriopheophytins-*a*/*b* (left) and synthetic bacteriochlorins (right).

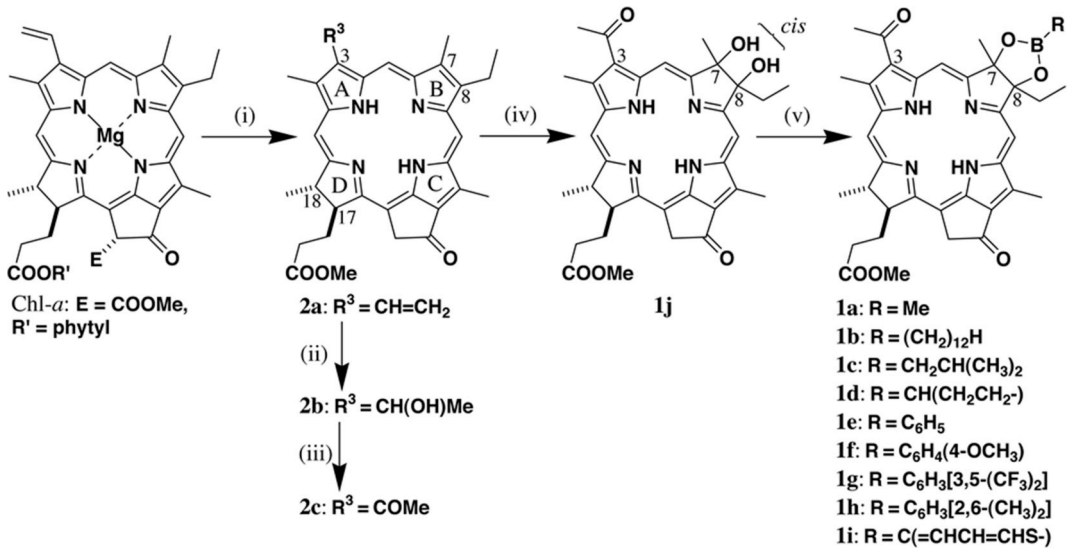

Scheme 1. Synthesis of methyl *cis*-7,8-dihydroxy-pyrobacteriopheophorbide-*a* (**1j**) and its boronates **1a–i** by chemical modification of naturally occurring Chl-*a*: (i) H_2SO_4/MeOH, rt and collidine, reflux; (ii) HBr/AcOH, H_2O/CH_2Cl_2, and CH_2N_2/Et_2O; (iii) $O(CH_2CH_2)_2NMeO–Pr_4NRuO_4/CH_2Cl_2$; (iv) $OsO_4–C_5H_5N/CH_2Cl_2$ and H_2S/MeOH; (v) $RB(OH)_2–MgSO_4$/dry THF or PhMe.

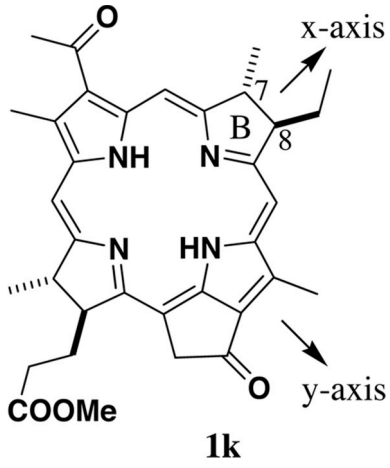

Fig. 2. Molecular structure of methyl pyrobacteriopheophorbide-*a* (**1k**) prepared from natural BChl-*a* with molecular x/y-axes.

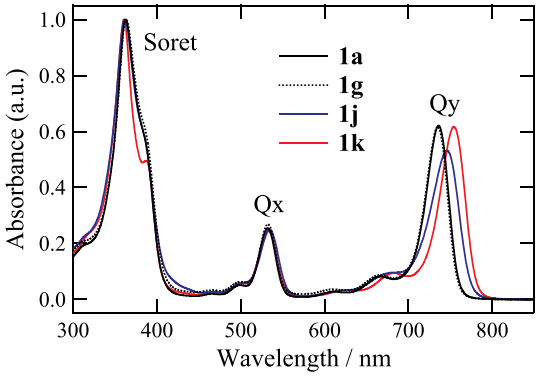

Fig. 3. Electronic absorption spectra of bacteriochlorins **1a/g/j/k** in dichloromethane (ca. 10 μM). All the spectra were normalized at their intense peaks in the Soret region.

with a *trans*-7,8-dihydrogenated form showed three maxima at 754 (Qy), 533 (Qx), and 361 nm (Soret) in dichloromethane, while *cis*-diol **1j** exhibited the corresponding maxima at 746, 535, and 362 nm. The transformation of *trans*-dihydrogenated to *cis*-dihydroxylated form at the 7,8-positions as in **1k** to **1j** induced a blue shift and broadening of the Qy bands: $\Delta\lambda_{abs} = 8$ nm and ΔFWHM(full width at half maximum) = 100 cm^{-1} (see Table 1). The broadening reduced the relative intensity (I_{rel}) of the Qy band over the major Soret band from 61% to 53%. The same modification resulted in a red shift of the Qx bands ($\Delta\lambda_{abs} = 2$ nm) and no significant change of the band shapes. By the structural alteration of **1k** to **1j**, the main Soret maxima slightly moved to a longer wavelength ($\Delta\lambda_{abs} = 1$ nm) and the band broadened apparently, whereas the minor Soret band at the red side shifted to a shorter wavelength (387 → ≈385 nm). The broadening of the main Soret band is comparable to that of the Qy bands, so the intense Soret band at a shorter wavelength would be assigned to the By band, and the Soret band at a longer wavelength could correspond to the Bx band. This characterization is consistent with the Gouterman's four-orbital model [28]: Qy, Qx, Bx, and By bands in a bacteriochlorin are situated from longer to shorter wavelengths.

Methylboronation of *cis*-diol **1j** to **1a** blue-shifted the Qy maxima by 10 nm and sharpened the band: ΔFWHM = −140 cm^{-1} and I_{rel} = 53% → 62% (see Fig. 3 and Table 1). The methylboronation also affected the Qx band in a similar manner, giving a small hypsochromic shift ($\Delta\lambda_{abs} = -3$

Table 1
Electronic absorption maxima λ_{abs} (nm) of bacteriochlorins **1a–k** in dichloromethane.

Compound (R)	Soret[a]	Qx[b]	Qy[b]
1a (Me)	363	532 (25) [830]	736 (62) [590]
1b ($C_{12}H_{25}$)	363	532 (25) [850]	737 (61) [600]
1c (iBu)	363	532 (25) [870]	736 (60) [600]
1d (cycloPr)	363	533 (25) [850]	737 (61) [600]
1e (Ph)	363	533 (26) [840]	736 (61) [600]
1f (Ph(4-OMe))	363	533 (26) [840]	736 (61) [600]
1g (Ph(3,5-$(CF_3)_2$))	363	533 (27) [850]	735 (62) [580]
1h (Ph(2,6-Me_2))	363	532 (26) [840]	736 (61) [590]
1i (2-thienyl)	363	533 (26) [850]	736 (61) [590]
1j	362	535 (25) [940]	746 (53) [730]
1k	361	533 (24) [910]	754 (61) [630]

[a] Main Soret maxima corresponding to By maxima.
[b] The values in parentheses and brackets indicate I_{rel} (%) and FWHM of bands (cm^{-1}), respectively.

nm) and sharpening of the band (ΔFWHM = −110 cm^{-1}). The Soret bands of **1a** exhibited a similar but slightly sharp shape as that of **1j**, and the main peak of the former was shifted to a longer wavelength by 1 nm than the latter. Comparing with the three bands of **1k**, **1a** showed a similar shape of the Qy band with a 18-nm blue shift, a slightly sharp Qx band with a small blue shift ($\Delta\lambda_{abs}$ = −1 nm), and a 2-nm red-shifted Soret maximum. The observed shifts are comparable to those by substitution with electron-withdrawing groups at the 7- or 8-position of chlorin π-skeleton reported previously [29,30]. Since the *cis*-7,8-dihydroxy moiety and its boronate as in **1a** and **1j**, respectively, were electron-withdrawing groups, the above substitution effect on electronic absorption bands could be explained by their electronic factor.

Substitution of the methyl group at the boron atom of **1a** with alkyl and aryl groups as in **1b–i** did not induce any apparent changes in the corresponding absorption spectra except for the Qy band of **1g** bearing a 3,5-bis(trifluoromethyl)phenyl group (see Fig. 3 and S1). The average values of absorption data of boronates **1a–i** with a standard deviation were calculated as follows (except for the Qy data of **1g**): λ_{abs}(Qy/Qx/Soret) = 736.2 ± 0.2/532.4 ± 0.2/362.9 ± 0.2 nm, I_{rel}(Qy/Qx) = 61.0 ± 0.6/25.6 ± 0.5, and FWHM(Qy/Qx) = 595 ± 4/846 ± 9 cm^{-1} (see Table 1). The effect of boronated substituents (R) on their electronic absorption spectra was limited, although the strong electron-withdrawing 3,5-bis(trifluoromethyl)phenyl group in **1g** slightly blue-shifted the Qy maximum ($\Delta\lambda_{abs}$ = −1 nm) and sharpened the Qy band (ΔFWHM = −15 cm^{-1}).

2.3. Fluorescence emission properties of boronated bacteriochlorins

Synthetic bacteriochlorins **1a–k** were highly fluorescent in a diluted dichloromethane solution. When **1k** was excited at the main Soret maxima (361 nm), fluorescence emission bands were observed as the mirror image of its Qy absorption bands (see the red line of Fig. 4). The main emission peak (λ_{em}) was located at 767 nm, and the Stokes shift (Δ) was 210 cm^{-1} (Table 2). The modification of the peripheral substituents at the B-ring from **1k** to **1j** resulted in an 8-nm blue shift of λ_{em} and a slight broadening of the main emission bands (ΔFWHM = 50 cm^{-1}). This fluorescence observation is comparable to the changes of their Qy absorption data (vide supra). By the above modification, the Stokes shift slightly enhanced (210 → 230 cm^{-1}), and the fluorescence emission quantum yields (Φ_{em}) rather reduced (16% → 14%).

The methylboronation of **1j** to **1a** induced a substantial blue shift of λ_{em} (759 → 747 nm) and sharpening of the emission band (FWHM = 550 → 490 cm^{-1}) (see Fig. 4 and Table 2), which corresponded to the changes of their Qy bands (vide supra). The Stokes shift decreased by the methylboronation (230 → 190 cm^{-1}). The suppression is ascribable to the conformational fixation of the 7,8-substituents by the boronated cyclization of the *cis*-diol. The Φ_{em} of **1a** was the same as that of **1j**.

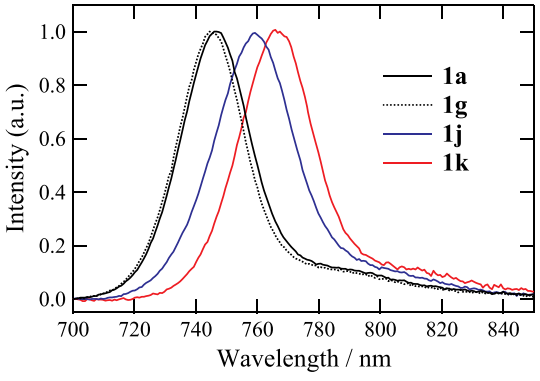

Fig. 4. Fluorescence emission spectra of bacteriochlorins **1a/g/j/k** in dichloromethane (ca. 1 μM, excitation at main Soret maxima). All the spectra were normalized at their intense peaks.

Table 2
Fluorescence emission data of bacteriochlorins **1a–k** in aerated dichloromethane at room temperature.[a]

Compound (R)	λ_{em}/nm[b]	Δ/cm^{-1}	Φ_{em}/%
1a (Me)	747 [490]	190	14
1b ($C_{12}H_{25}$)	747 [490]	200	18
1c (iBu)	747 [490]	210	16
1d (cycloPr)	748 [490]	210	17
1e (Ph)	748 [490]	210	13
1f (Ph(4-OMe))	747 [480]	200	18
1g (Ph(3,5-$(CF_3)_2$))	745 [470]	190	19
1h (Ph(2,6-Me_2))	747 [490]	200	14
1i (2-thienyl)	747 [480]	200	18
1j	759 [550]	230	14
1k	767 [500]	210	16

[a] λ_{em}, emission maximum (excited at Soret maxima); Δ, Stokes shift = [1/λ_{abs}(Qy) − 1/λ_{em}] x 10^7; Φ_{em}, emission quantum yield (excited at main Soret maxima).
[b] The values in brackets indicate FWHM of bands (cm^{-1}).

Similarly as in the changes of the Qy bands, the shapes of the emission bands of **1a** and **1k** were the same, and the λ_{em} of **1a** significantly moved to a shorter wavelength by 20 nm than that of **1k**. Both the Stokes shift and Φ_{em} of **1a** were slightly smaller than those of **1k**.

The λ_{em} and FWHM values of boronates **1a–i** were independent of the substituents (R) except for **1g** (see Table 2 and Fig. S2), as aforementioned for their Qy absorption data. The average value of the λ_{em} of **1a–f/h/i** is 747.3 ± 0.4 nm and larger than 745 nm for **1g**, while the mean FWHM of the formers is 488 ± 4 cm^{-1} and larger than 470 cm^{-1} for the latter. The slightly blue-shifted and sharp emission band was observed in **1g** (Fig. 4). The Stokes shifts of all boronates **1a–i** are comparable to each other, giving 200 ± 7 cm^{-1} for the average value. These small values indicate that the structural difference between their ground and excited states is not so large. Their Φ_{em} values partially fluctuated, and **1g** gave the maximum value of 19%. Therefore, the effect of the R groups on the fluorescence properties is limited.

3. Experimental

3.1. General

Electronic absorption spectra were measured with a Hitachi U-3500 spectrophotometer. The fluorescence emission spectra and quantum yields excited at Soret maxima were obtained by a Hamamatsu Photonics C9920-03G spectrometer. ^{1}H NMR spectra were recorded on a JEOL ECA-600 (600 MHz) or AL400 (400 MHz) spectrometer; residual $CHCl_3$ (δ = 7.26 ppm) was used as an internal reference. High resolution mass spectra (HRMS) were recorded on a Bruker micrOTOF II spectrometer: atmospheric pressure chemical ionization (APCI) and positive mode in a methanol solution. FCC and TLC were performed with silica gel (Wakogel C-300 and Merck Kieselgel 60 F_{254}).

Methyl 7,8-didehydro-*cis*-7,8-dihydroxy-pyrobacteriopheophorbide-*a* (**1j**) [26] and methyl pyrobacteriopheophorbide-*a* (**1k**) [14] were prepared according to reported procedures. All the reaction reagents and solvents were obtained from commercial suppliers and utilized as supplied. Dry THF and toluene was obtained by reflux with calcium chloride and distillation. Dichloromethane for optical spectroscopy was purchased from Nacalai Tesque as a reagent prepared specially for spectroscopy and used without further purification.

3.2. Synthetic procedures for boronation

A 1:1 7,8-diastereomeric mixture of *cis*-diol **1j** (9.0 mg, 15 μmol) was dissolved in dry THF or toluene (15 ml), to which were added boronic acids (90 μmol, 6 eq) and magnesium sulfate (2.4 mg, 20 μmol). The mixture was stirred at room temperature or refluxed under nitrogen in the dark. After the starting diol was consumed (monitored by TLC), the

reaction mixture was filtrated, the solvent was evaporated, and the residue was purified by FCC (0–1% MeOH/CH_2Cl_2 or 0–10% Et_2O/CH_2Cl_2) and recrystallization (CH_2Cl_2/hexane) to give a (7*R*,8*S*)- and (7*S*,8*R*)-diastereomeric mixture of the corresponding boronates **1a–i** as black solid (see their spectral data below and their ^{1}H NMR spectra in Figs. S3–S11): isolated yields = 80% (**1a**: R = Me, THF, reflux, 1 d, 1:1 stereoisomers), 90% (**1b**: dodecyl, toluene, reflux, 2 h, 1:1), 81% (**1c**: isobutyl, toluene, reflux, 2 h, 1:1), 34% (**1d**: cyclopropyl, toluene, reflux, 1 d, 1:1), 77% (**1e**: phenyl, THF, rt, 2 d, 1:1), 97% (**1f**: *p*-anisyl, THF, rt, 1 d, 1:1), 78% (**1g**: 3,5-bis(trifluoromethyl)phenyl, toluene, reflux, 2 h, 1:1), 73% (**1h**: 2,6-dimethylphenyl, toluene, reflux, 1 d, 5:4), and 51% (**1i**: 2-thienyl, toluene, reflux, 1 h, 1:1).

3.3. Spectral data of boronates

3.3.1. Methylboronate of methyl 7,8-didehydro-cis-7,8-dihydroxy-pyrobacteriopheophorbide-a (1a)

UV-VIS (CH_2Cl_2) λ_{max} 363 (ε, 100,000), 532 (25,000), 736 nm (62,000); ^{1}H NMR (600 MHz, $CDCl_3$) δ(1/1) 9.32/9.28 (1H, s, 5-H), 8.83/8.82 (1H, s, 10-H), 8.57/8.56 (1H, s, 20-H), 5.15, 5.02/5.00 (each 1H, d, J = 20 Hz, 13^1-CH_2), 4.38/4.36 (1H, dq, J = 2, 7 Hz, 18-H), 4.21/4.19 (1H, dt, J = 7, 2 Hz, 17-H), 3.63/3.62 (3H, s, 17^2-$COOCH_3$), 3.541/3.535 (3H, s, 2-CH_3), 3.53/3.52 (3H, s, 12-CH_3), 3.21 (3H, s, 3^1-CH_3), 2.85–2.74 (2H, m, 8-CH_2), 2.66–2.61, 2.58–2.50 (each 1H, m, 17^1-CH_2), 2.40/2.37 (3H, s, 7-CH_3), 2.32–2.21 (2H, m, 17-CH_2), 1.755/1.752 (3H, d, J = 7 Hz, 18-CH_3), 0.96/0.88 (3H, t, J = 7 Hz, 8^1-CH_3), 0.27 (3H, s, BCH_3), −0.13/–0.20, −1.43/–1.46 (each 1H, s, NH x 2); HRMS (APCI) found: *m/z* 623.3042, calcd for $C_{35}H_{40}N_4O_6B$: MH^+, 623.3035.

3.3.2. 1-Dodecylboronate of methyl 7,8-didehydro-cis-7,8-dihydroxy-pyrobacteriopheophorbide-a (1b)

UV-VIS (CH_2Cl_2) λ_{max} 363 (I_{rel}, 100), 532 (25), 737 nm (61); ^{1}H NMR (600 MHz, $CDCl_3$) δ(1/1) 9.30/9.26 (1H, s, 5-H), 8.82/8.81 (1H, s, 10-H), 8.56/8.55 (1H, s, 20-H), 5.15, 5.01/4.99 (each 1H, d, J = 19 Hz, 13^1-CH_2), 4.38/4.36 (1H, dq, J = 2, 7 Hz, 18-H), 4.20/4.19 (1H, dt, J = 7, 2 Hz, 17-H), 3.629/3.627 (3H, s, 17^2-$COOCH_3$), 3.54, 3.53, 3.53, 3.52 (each half of 3H, s, 2-, 12-CH_3), 3.21 (3H, s, 3^1-CH_3), 2.88–2.73 (2H, m, 8-CH_2), 2.67–2.51 (2H, m, 17^1-CH_2), 2.37/2.34 (3H, s, 7-CH_3), 2.32–2.20 (2H, m, 17-CH_2), 1.754/1.749 (3H, d, J = 7 Hz, 18-CH_3), 1.40–1.00 (20H, m, $BC(CH_2)_{10}$), 0.97/0.89 (3H, t, J = 8 Hz, 8^1-CH_3), 0.844/0.840 (3H, t, J = 7 Hz, $BC_{11}CH_3$), 0.77 (2H, t, J = 8 Hz, BCH_2), −0.08/–0.15, −1.39/–1.43 (each 1H, s, NH x 2); HRMS (APCI) found: *m/z* 777.4766, calcd for $C_{46}H_{62}N_4O_6B$: MH^+, 777.4757.

3.3.3. Isobutylboronate of methyl 7,8-didehydro-cis-7,8-dihydroxy-pyrobacteriopheophorbide-a (1c)

UV-VIS (CH_2Cl_2) λ_{max} 363 (I_{rel}, 100), 532 (25), 736 nm (60); ^{1}H NMR (600 MHz, $CDCl_3$) δ(1/1) 9.30/9.26 (1H, s, 5-H), 8.82/8.81 (1H, s, 10-H), 8.56/8.55 (1H, s, 20-H), 5.15, 5.01/4.99 (each 1H, d, J = 19 Hz, 13^1-CH_2), 4.38/4.36 (1H, dq, J = 2, 7 Hz, 18-H), 4.20/4.18 (1H, dt, J = 7, 2 Hz, 17-H), 3.63/3.62 (3H, s, 17^2-$COOCH_3$), 3.535, 3.528, 3.527, 3.517 (each half of 3H, s, 2-, 12-CH_3), 3.21 (3H, s, 3^1-CH_3), 2.85–2.72 (2H, m, 8-CH_2), 2.66–2.50 (2H, m, 17^1-CH_2), 2.37/2.34 (3H, s, 7-CH_3), 2.32–2.20 (2H, m, 17-CH_2), 1.85–1.77 (1H, m, BCCH), 1.752/1.749 (3H, d, J = 7 Hz, 18-CH_3), 0.98/0.89 (3H, t, J = 8 Hz, 8^1-CH_3), 0.78–0.74 (8H, m, $BCH_2C(CH_3)_2$), −0.09/–0.16, −1.40/–1.44 (each 1H, s, NH x 2); HRMS (APCI) found: *m/z* 665.3508, calcd for $C_{38}H_{46}N_4O_6B$: MH^+, 665.3505.

3.3.4. Cyclopropylboronate of methyl 7,8-didehydro-cis-7,8-dihydroxy-pyrobacteriopheophorbide-a (1d)

UV-VIS (CH_2Cl_2) λ_{max} 363 (I_{rel}, 100), 533 (25), 737 nm (61); ^{1}H NMR (400 MHz, $CDCl_3$) δ(1/1) 9.27/9.22 (1H, s, 5-H), 8.79/8.78 (1H, s, 10-H), 8.56/8.54 (1H, s, 20-H), 5.15/5.14, 5.01/4.99 (each 1H, d, J = 20 Hz, 13^1-CH_2), 4.38–4.34 (1H, m, 18-H), 4.21–4.18 (1H, m, 17-H), 3.63/3.62 (3H, s, 17^2-$COOCH_3$), 3.53, 3.52, 3.52, 3.51 (each half of 3H, s, 2-, 12-CH_3), 3.21 (3H, s, 3^1-CH_3), 2.84–2.69 (2H, m, 8-CH_2), 2.67–2.51 (2H, m, 17^1-CH_2), 2.33/2.30 (3H, s, 7-CH_3), 2.28–2.22 (2H, m, 17-CH_2), 1.75 (3H, d, J = 7 Hz, 18-CH_3), 0.97/0.88 (3H, t, J = 8 Hz, 8^1-CH_3), 0.53–0.45 (4H, m, $BC(CH_2)_2$), −0.07/–0.14, −1.38/–1.42 (each 1H, s, NH x 2), −0.2 (1H, m, BCH); HRMS (APCI) found: *m/z* 649.3194, calcd for $C_{37}H_{42}N_4O_6B$: MH^+, 649.3192.

3.3.5. Phenylboronate of methyl 7,8-didehydro-cis-7,8-dihydroxy-pyrobacteriopheophorbide-a (1e)

UV-VIS (CH_2Cl_2) λ_{max} 363 (ε, 100,000), 533 (26,000), 736 nm (61,000); ^{1}H NMR (400 MHz, $CDCl_3$) δ(1/1) 9.41/9.37 (1H, s, 5-H), 8.90/8.89 (1H, s, 10-H), 8.56/8.54 (1H, s, 20-H), 7.84 (2H, dt, J = 8, 1 Hz, Ph-2,6-H), 7.36 (1H, tt, J = 8, 1 Hz, Ph-4-H), 7.27 (2H, br-t, J = 8 Hz, Ph-3,5-H), 5.15/5.14, 5.00/4.98 (each 1H, d, J = 20 Hz, 13^1-CH_2), 4.40–4.32 (1H, m, 18-H), 4.21–4.16 (1H, m, 17-H), 3.63/3.60 (3H, s, 17^2-$COOCH_3$), 3.552/3.543 (3H, s, 12-CH_3), 3.542/3.532 (3H, s, 2-CH_3), 3.235/3.233 (3H, s, 3^1-CH_3), 2.96–2.82 (2H, m, 8-CH_2), 2.67–2.48 (2H, m, 17^1-CH_2), 2.46/2.43 (3H, s, 7-CH_3), 2.32–2.18 (2H, s, 17-CH_2), 1.75 (3H, d, J = 8 Hz, 18-CH_3), 1.04/0.95 (3H, t, J = 8 Hz, 8^1-CH_3), −0.07/–0.15, −1.38/–1.43 (each 1H, s, NH x 2); HRMS (APCI) found: *m/z* 685.3199, calcd for $C_{40}H_{42}N_4O_6B$: MH^+, 685.3192.

3.3.6. p-Anisylboronate of methyl 7,8-didehydro-cis-7,8-dihydroxy-pyrobacteriopheophorbide-a (1f)

UV-VIS (CH_2Cl_2) λ_{max} 363 (I_{rel}, 100), 533 (26), 736 nm (61); ^{1}H NMR (400 MHz, $CDCl_3$) δ(1/1) 9.39/9.35 (1H, s, 5-H), 8.89/8.88 (1H, s, 10-H), 8.55/8.53 (1H, s, 20-H), 7.79/7.78 (2H, d, J = 8 Hz, *o*-H x 2), 6.80 (2H, d, J = 8 Hz, *m*-H x 2), 5.15/5.14, 5.00/4.98 (each 1H, d, J = 20 Hz, 13^1-CH_2), 4.38–4.33 (1H, m, 18-H), 4.19–4.17 (1H, m, 17-H), 3.73 (3H, s, *p*-OCH_3), 3.63/3.60 (3H, s, 17^2-$COOCH_3$), 3.55, 3.54, 3.54, 3.53 (each half of 3H, s, 2-, 12-CH_3), 3.23 (3H, s, 3^1-CH_3), 2.95–2.81 (2H, m, 8-CH_2), 2.67–2.48 (2H, m, 17^1-CH_2), 2.44/2.41 (3H, s, 7-CH_3), 2.32–2.21 (2H, m, 17-CH_2), 1.74 (3H, d, J = 7 Hz, 18-CH_3), 1.03/0.94 (3H, t, J = 7 Hz, 8^1-CH_3), −0.05/–0.13, −1.37/–1.41 (each 1H, s, NH x 2); HRMS (APCI) found: *m/z* 715.3302, calcd for $C_{41}H_{44}N_4O_7B$: MH^+, 715.3298.

3.3.7. 3,5-Bis(trifluoromethyl)phenylboronate of methyl 7,8-didehydro-cis-7,8-dihydroxy-pyrobacteriopheophorbide-a (1g)

UV-VIS (CH_2Cl_2) λ_{max} 363 (I_{rel}, 100), 533 (27), 735 nm (62); ^{1}H NMR (400 MHz, $CDCl_3$) δ(1/1) 9.47/9.43 (1H, s, 5-H), 8.91/8.90 (1H, s, 10-H), 8.60/8.58 (1H, s, 20-H), 8.26 (2H, s, Ph-2,6-H), 7.85 (1H, s, Ph-4-H), 5.16, 5.02/5.00 (each 1H, d, J = 20 Hz, 13^1-CH_2), 4.41–4.34 (1H, m, 18-H), 4.21–4.19 (1H, m, 17-H), 3.63/3.60 (3H, s, 17^2-$COOCH_3$), 3.58, 3.57, 3.57, 3.56 (each half of 3H, s, 2-, 12-CH_3), 3.25 (3H, s, 3^1-CH_3), 2.96–2.88 (2H, m, 8-CH_2), 2.67–2.53 (2H, m, 17^1-CH_2), 2.51/2.48 (3H, s, 7-CH_3), 2.32–2.17 (2H, m, 17-CH_2), 1.76/1.75 (3H, d, J = 7 Hz, 18-CH_3), 1.03/0.95 (3H, t, J = 7 Hz, 8^1-CH_3), −0.17/–0.24, −1.44/–1.48 (each 1H, s, NH x 2); HRMS (APCI) found: *m/z* 821.2950, calcd for $C_{42}H_{40}N_4O_6BF_6$: MH^+, 821.2940.

3.3.8. 2,6-Dimethylphenylboronate of methyl 7,8-didehydro-cis-7,8-dihydroxy-pyrobacteriopheophorbide-a (1h)

UV-VIS (CH_2Cl_2) λ_{max} 363 (I_{rel}, 100), 532 (26), 736 nm (61); ^{1}H NMR (400 MHz, $CDCl_3$) δ(5/4) 9.38/9.35 (1H, s, 5-H), 8.90/8.89 (1H, s, 10-H), 8.60/8.58 (1H, s, 20-H), 7.033/7.028 (1H, t, J = 8 Hz, Ph-4-H), 6.81/6.80 (2H, d, J = 8 Hz, Ph-3,5-H), 5.17/5.16, 5.02/4.99 (each 1H, d, J = 20 Hz, 13^1-CH_2), 4.41–4.38 (1H, m, 18-H), 4.23–4.20 (1H, m, 17-H), 3.62/3.64 (3H, s, 17^2-$COOCH_3$), 3.55/3.54 (3H, s, 2-CH_3), 3.53/3.52 (3H, s, 12-CH_3), 3.199/3.195 (3H, s, 3^1-CH_3), 2.92–2.82 (2H, m, 8-CH_2), 2.65–2.54 (2H, m, 17^1-CH_2), 2.51/2.49 (3H, s, 7-CH_3), 2.35–2.24 (2H, m, 17-CH_2), 2.06/2.04 (6H, s, Ph-2,6-CH_3), 1.76/1.78 (3H, d, J = 7 Hz, 18-CH_3), 0.93/1.02 (3H, t, J = 8 Hz, 8^1-CH_3), −0.17/–0.11, −1.44/–1.41 (each 1H, s, NH x 2); HRMS (APCI) found: *m/z* 713.3512, calcd for $C_{42}H_{46}N_4O_6B$: MH^+, 713.3505.

*3.3.9. 2-Thienylboronate of methyl 7,8-didehydro-cis-7,8-dihydroxy-pyrobacteriopheophorbide-a (**1i**)*

UV-VIS (CH_2Cl_2) λ_{max} 363 (I_{rel}, 100), 533 (26), 736 nm (61); ^{1}H NMR (600 MHz, $CDCl_3$) δ(1/1) 9.39/9.35 (1H, s, 5-H), 8.90/8.89 (1H, s, 10-H), 8.56/8.54 (1H, s, 20-H), 7.67 (1H, m, thienyl-5-H), 7.55 (1H, d, J = 4 Hz, thienyl-3-H), 7.09 (1H, t, J = 4 Hz, thienyl-4-H), 5.15/5.14, 5.00/4.99 (each 1H, d, J = 19 Hz, 13^1-CH_2), 4.39–4.33 (1H, m, 18-H), 4.21–4.17 (1H, m, 17-H), 3.63/3.60 (3H, s, 17^2-$COOCH_3$), 3.55, 3.54, 3.54, 3.53 (each half of 3H, s, 2-, 12-CH_3), 3.23 (3H, s, 3^1-CH_3), 2.95–2.84 (2H, m, 8-CH_2), 2.65–2.51 (2H, m, 17^1-CH_2), 2.47/2.43 (3H, s, 7-CH_3), 2.32–2.22 (2H, m, 17-CH_2), 1.75 (3H, d, J = 8 Hz, 18-CH_3), 1.02/0.93 (3H, t, J = 8 Hz, 8^1-CH_3), −0.10/–0.18, −1.40/–1.45 (each 1H, s, NH x 2); HRMS (APCI) found: *m/z* 691.2764, calcd for $C_{38}H_{40}N_4O_6BS$: MH^+, 691.2756.

Declaration of competing interest

The authors declare no conflict of interest.

CRediT authorship contribution statement

Daichi Funakoshi: Investigation, Visualization. **Yosaku Nomura:** Investigation. **Sunao Shoji:** Investigation. **Hitoshi Tamiaki:** Conceptualization, Writing - original draft, Supervision, Project administration, Funding acquisition.

Acknowledgements

This work was partially supported by Japan Society for the Promotion of Science (JSPS) KAKENHI Grant Number JP17H06436 in Scientific Research on Innovative Areas “Innovation for Light-Energy Conversion (I^4LEC)".

Appendix A. Supplementary data

Supplementary data to this article can be found online at https://doi.org/10.1016/j.dyepig.2019.108155.

References

[1] Deisenhofer J, Epp O, Miki K, Huber R, Michel H. Nature 1985;318:618–24.
[2] Feher G, Allen JP, Okamura MY, Rees DC. Nature 1989;339:111–6.
[3] Yu L-J, Suga M, Wang-Otomo Z-Y, Shen J-R. Nature 2018;556:209–13.
[4] Tamiaki H, Shibata R, Mizoguchi T. Photochem Photobiol 2007;83:152–62.
[5] Ward LM, Cardona T, Holland-Moritz H. Front Microbiol 2019;10:1658.
[6] Wang X-F, Tamiaki H. Energy Environ Sci 2010;3:94–106.
[7] Duan S, Chen G, Li M, Chen G, Wang X-F, Tamiaki H, Sasaki S. J Photochem Photobiol A Chem 2017;347:49–54.
[8] Panchenko PA, Grin MA, Fedorova OA, Zakharko MA, Pitmov DA, Mironov AF, Arkhipova AN, Fedorov YV, Jonusauskas G, Yakubovskaya RI, Morozova NB, Ignatova AA, Feofanov AV. Phys Chem Chem Phys 2017;19:30195–206.
[9] Zhu W, Gao Y-H, Liao P-Y, Chen D-Y, Sun N-N, Thi PAN, Yan Y-J, Wu X-F, Chen Z-L. Eur J Med Chem 2018;160:146–56.
[10] Ogata F, Nagaya T, Maruoka Y, Akhigbe J, Meares A, Lucero MY, Satraitis A, Fujimura D, Okada R, Inagaki F, Choyke PL, Ptaszek M, Kobayashi H. Bioconjug Chem 2019;30:169–83.
[11] Overchuk M, Zheng M, Rajora MA, Charron DM, Chen J, Zheng G. ACS Nano 2019;13:4560–71.
[12] Harmatys KM, Overchuk M, Zheng G. Acc Chem Res 2019;52:1265–74.
[13] Zhang K, Yu Z, Meng X, Zhao W, Shi Z, Yang Z, Dong H, Zhang X. Adv Sci 2019;6:1900530.
[14] Tamiaki H, Kouraba M, Takeda K, Kondo S, Tanikaga R. Tetrahedron: Asymmetry 1998;9:2101–11.
[15] Kunieda M, Mizoguchi T, Tamiaki H. Tetrahedron 2004;60:11349–57.
[16] Kunieda M, Tamiaki H. J Org Chem 2005;70:820–8.
[17] Ponsot F, Debois N, Bucher L, Berthelot M, Mondal P, Gros CP, Romieu A. Dyes Pigments 2019;160:747–56.
[18] Meares A, Yu Z, Bhagavathy GV, Satraitis A, Ptaszek M. J Org Chem 2019;84:7851–62.
[19] Yao Y, Rao Y, Liu Y, Jiang L, Xiong J, Fan Y-J, Shen Z, Sessler JL, Zhang J-L. Phys Chem Chem Phys 2019;21:10152–62.
[20] Zhang S, Lindsey JS. J Org Chem 2017;82:2489–504.
[21] Kozyrev AN, Chen Y, Goswami LN, Tabaczynski WA, Pandey RK. J Org Chem 2006;71:1949–60.
[22] Kunieda M, Yamamoto K, Sasaki S, Tamiaki H. Chem Lett 2007;36:936–7.
[23] Tamiaki H, Takeuchi S, Tsudzuki S, Miyatake T, Tanikaga R. Tetrahedron 1998;54:6699–718.
[24] Smith KM, Bisset GMF, Bushell MJ. J Org Chem 1980;45:2218–24.
[25] Tamiaki H, Yagai S, Miyatake T. Bioorg Med Chem 1998;6:2171–8.
[26] Sasaki S, Omoda M, Tamiaki H. J Photochem Photobiol A Chem 2004;162:307–15.
[27] Takao N, Suto A, Kondo Y, Ishihara K. Inorg Chim Acta 1999;290:222–7.
[28] Gouterman M. J Mol Spectrosc 1961;6:138–63.
[29] Tamiaki H, Kunieda M. Handbook Porphyrin Sci 2011;10:223–90.
[30] Tamiaki H, Tanaka T. Tetrahedron 2015;71:1915–23.